

## SYNTHESIS AND CHARACTERISATION OF $\text{Ni}_{0.25}\text{Co}_{0.75}\text{Fe}_2\text{O}_4$ NANOSTRUCTURES

K. Kalpanadevi, C.R. Sinduja and R. Manimekalai\*

Department of Chemistry, Kongunadu Arts and Science College, Coimbatore, Tamilnadu  
PIN – 641 029, India

(Received November 9, 2013; revised September 2, 2015)

**ABSTRACT.** The synthesis of  $\text{Ni}_{0.25}\text{Co}_{0.75}\text{Fe}_2\text{O}_4$  nanoparticles has been achieved by a simple thermal decomposition method from the inorganic precursor,  $\text{Ni}_{0.25}\text{Co}_{0.75}\text{Fe}_2(\text{cin})_3(\text{N}_2\text{H}_4)_5$ , which was obtained by a novel precipitation method from the corresponding metal salts, cinnamic acid and hydrazine hydrate. The precursor was characterised by hydrazine and metal analyses, infrared spectral analysis and thermo gravimetric analysis. On appropriate annealing,  $\text{Ni}_{0.25}\text{Co}_{0.75}\text{Fe}_2(\text{cin})_3(\text{N}_2\text{H}_4)_5$  yielded  $\text{Ni}_{0.25}\text{Co}_{0.75}\text{Fe}_2\text{O}_4$  nanoparticles, which were characterised for their size and structure using X-ray diffraction (XRD), high resolution transmission electron microscopic (HRTEM), selected area electron diffraction (SAED) and scanning electron microscopic (SEM) techniques.

**KEY WORDS:**  $\text{Ni}_{0.25}\text{Co}_{0.75}\text{Fe}_2\text{O}_4$  nanoparticles, XRD, HRTEM, SAED, SEM

### INTRODUCTION

Nanocrystalline ferrites, an important class of magnetic materials, have impressed the researchers in the recent past, due to their unique properties like significant saturation magnetization, moderate to high permittivity, high electrical resistivity, low electrical losses and very good chemical stability, which are markedly different from those of their micrometer-sized counterparts. For many applications, ferrites cannot be replaced with ferromagnetic metals, as the former compete with the latter on economic grounds. Nano-scale ferrites are associated with revolutionary applications in the field of electronic technology as well as biotechnology [1]. Nickel doped cobalt ferrites are technologically important nowadays as they are found to be suitable for high frequency applications [2], gas sensors [3], etc.

To date, a wide variety of methods are employed for the synthesis of ferrites in their nano-scale, such as, sol-gel method [4], co-precipitation [5], ceramic technique [6], hydrothermal method [7], solvothermal method [8], etc. However, all the above said methods may have their own disadvantages like complicated procedure, usage of non-green solvents, need of very high processing temperature and expensive equipments, production of particles with uncontrolled morphologies, etc., Recently, thermal decomposition method has attained considerable interest due to its simple process, low cost, products with high purity and crystallinity and a larger surface area of the as-prepared particles.

Thermal treatment of suitable precursors containing metal or mixed metal formate [9], oxalate [10], acetate and propionate [11], malate [12], malonate, succinate and itaconates [13, 14], maleate and tartrate [15, 16] and fumarate [17-19] hydrazinates has been effectively employed in the synthesis of ferrite nanoparticles in the past years. A more recent work of us dealt with the synthesis of nano ferrite from an inorganic precursor containing phenyl acetate [20] hydrazinate. In this work, we have made an attempt to synthesise nickel doped cobalt ferrite nanoparticles via thermal decomposition route from the precursor containing the corresponding metal cinnamate hydrazinate.

\*Corresponding author. E-mail: manimekalaikase@gmail.com

## EXPERIMENTAL

### *Method of preparation and characterisation of the precursor $Ni_{0.25}Co_{0.75}Fe_2(cin)_3(N_2H_4)_5$*

This was prepared by the addition of an aqueous solution (50 mL) of hydrazine hydrate (1.6 mL, 30 mmol) and cinnamic acid (1.18 g, 0.79 mmol) to the corresponding aqueous solution (50 mL) of cobalt nitrate hexahydrate (0.4656 g, 1.5 mmol), nickel nitrate hexahydrate (0.23 g, 0.7 mmol) and ferrous sulfate heptahydrate (1.11 g, 3.9 mmol). After complete reaction, a brown orange product formed was kept aside for an hour for digestion, then filtered and washed with water, alcohol followed by diethylether and air dried.

The hydrazine content in the precursor was determined by titration using  $KIO_3$  as the titrant under Andrew's condition [21]. The percentage of nickel, cobalt and iron in the precursor was estimated by gravimetry as given in the Vogel's textbook [21]. The infrared spectrum of the solid precursor sample was recorded by the KBr disc technique using a Shimadzu spectrophotometer. The simultaneous TG-DSC experiment was carried out in Universal V4.5A TA Instrument, in nitrogen atmosphere at the heating rate of 20 °C per min using 5-10 mg of the sample. The temperature range was ambient to 700 °C.

### *Method of preparation and characterisation of $Ni_{0.25}Co_{0.75}Fe_2O_4$ nanoparticles*

$Ni_{0.25}Co_{0.75}Fe_2O_4$  nanoparticles were obtained from the autocatalytic decomposition of the precursor. In this method, the dried precursor was transferred to a silica crucible and heated to red hot condition in an ordinary atmosphere for about 45 min. The precursor started decomposing violently. A black powder was obtained at the end of the whole process, which was cooled down to room temperature by removing the heat source. It was ground well and stored in a desiccator. The particle size of the synthesised nanoparticles was determined by high resolution transmission electron microscopy (HRTEM) operating on Jeol Jem 2100 advanced analytical electron microscope. Scanning electron microscopy (SEM) was performed with a HITACHI Model S-3000H by focusing on nanoparticles to study the morphology. To check phase formation and purity, XRD pattern was recorded using an X-ray diffractometer (X'per PRO model) using  $CuK_{\alpha}$  radiation, at 40 keV.

## RESULTS AND DISCUSSION

### *Chemical formula determination of the precursor*

Based on the observed percentage of hydrazine (20.23), nickel (6.19), cobalt (19.09) and iron (46.97) which are found to match closely with the calculated values (20.84), (6.25), (18.84) and (47.61) for hydrazine, nickel, cobalt and iron, respectively, the chemical formula  $Ni_{0.25}Co_{0.75}Fe_2(cin)_3(N_2H_4)_5$  has been tentatively assigned to the precursor.

### *IR spectral analysis of the precursor*

The IR spectrum of  $Ni_{0.25}Co_{0.75}Fe_2(cin)_3(N_2H_4)_5$  displays an intensive band is observed at 972  $cm^{-1}$  due to the N-N stretching frequency, which unambiguously proves the bidentate bridging nature of the hydrazine ligand [22]. The asymmetric and symmetric stretching frequencies of the carboxylate ions are seen at 1639 and 1411  $cm^{-1}$ , respectively with the  $\Delta\nu$  ( $\nu_{asym} - \nu_{sym}$ ) separation of 228  $cm^{-1}$ , which strongly suggest the monodentate linkage of the carboxylate groups. The peak at 3367  $cm^{-1}$  corresponds to the N-H stretching vibration.

*Thermal analysis of the precursor*

The TG curve in Figure 1 shows that the precursor loses weight in three particular steps. The first step which is a minor weight loss step (20%) (theoretical loss of 19.8%) is related to the removal of the hydrazine molecules between room temperature and 190 °C. The corresponding peak in DSC is observed as an exotherm. The second step is associated with the total decarboxylation of the dehydrazinated precursor with a weight loss of 22%, (theoretical loss of 22.2%). The last step at 347 °C corresponds to the formation  $\text{Ni}_{0.25}\text{Co}_{0.75}\text{Fe}_2\text{O}_4$  as the final residue.

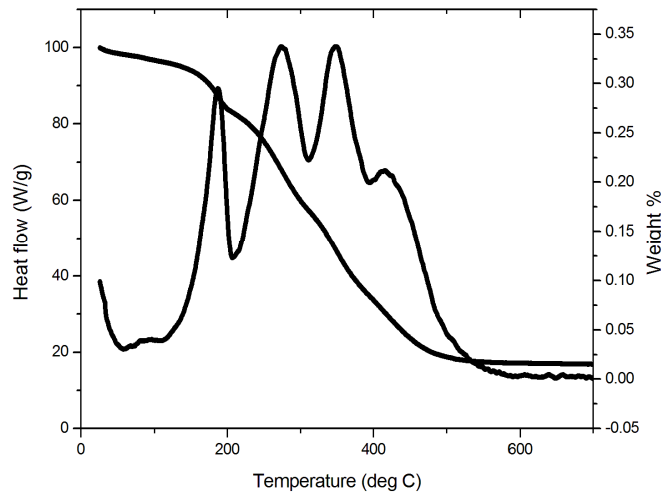


Figure 1. TG-DSC curve of  $\text{Ni}_{0.25}\text{Co}_{0.75}\text{Fe}_2(\text{cin})_3(\text{N}_2\text{H}_4)_5$ .

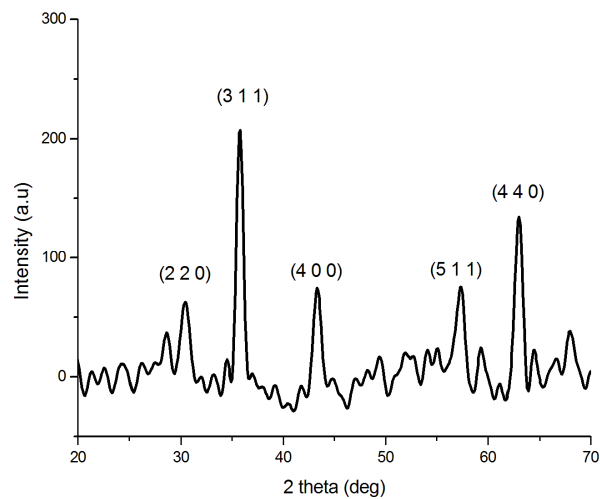
*Characterisation of  $\text{Ni}_{0.25}\text{Co}_{0.75}\text{Fe}_2\text{O}_4$  nanoparticles*

Figure 2. XRD pattern of  $\text{Ni}_{0.25}\text{Co}_{0.75}\text{Fe}_2\text{O}_4$  nanoparticles.

*XRD analysis*

XRD pattern of  $\text{Ni}_{0.25}\text{Co}_{0.75}\text{Fe}_2\text{O}_4$  nanoparticles is shown in Figure 2. The diffraction pattern of the sample shows broad peaks, indicating the fine crystalline nature of the particles. The cubic spinel structure of the sample is confirmed by the most intense peak (3 1 1) [23]. The results obtained from XRD are in good agreement with the JCPDS card of  $\text{Ni}_{(1-x)}\text{Co}_x\text{Fe}_2\text{O}_4$  (22-1086) [24] and JCPDS card (74-2081) [25]. The average crystallite size calculated by applying Scherrer formula,  $D = K\lambda / \beta \cos\theta$ , where,  $\theta$  is Bragg diffraction angle,  $K$  is constant,  $\lambda$  is the source wavelength (1.54), and  $\beta$  is the width of the XRD peak at half maximum height, is found to be 11 nm.

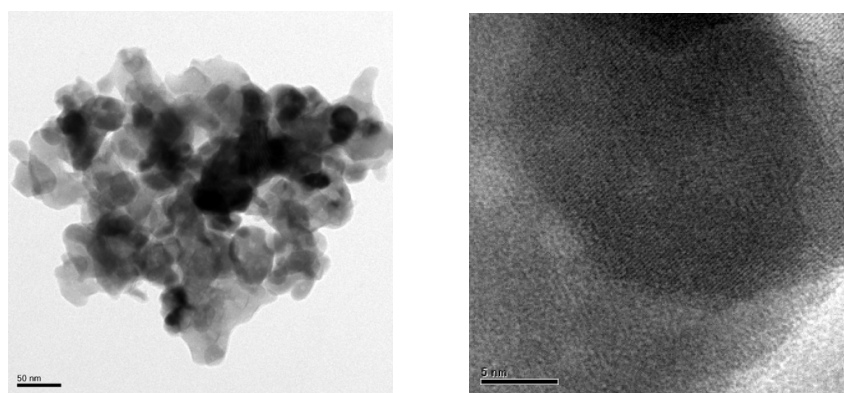


Figure 3. HRTEM image of  $\text{Ni}_{0.25}\text{Co}_{0.75}\text{Fe}_2\text{O}_4$  nanoparticles.

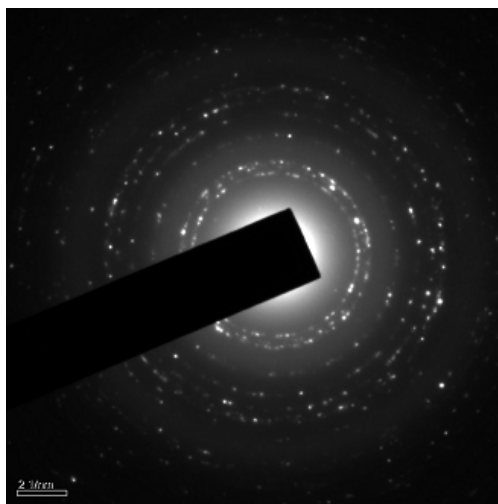


Figure 4. SAED pattern of  $\text{Ni}_{0.25}\text{Co}_{0.75}\text{Fe}_2\text{O}_4$  nanoparticles.

*HRTEM analysis*

HRTEM micrographs of  $\text{Ni}_{0.25}\text{Co}_{0.75}\text{Fe}_2\text{O}_4$  are shown in Figure 3, which show that the nanoparticles are of quite uniform polydispersed spherical shape. The presence of some bigger particles should be attributed to be the aggregation or overlapping of some small particles. It is clearly seen from the HRTEM bright field images that the sample consists of crystallites with particle sizes around 12 nm, which concurs with the results of XRD. Figure 4 shows the selected area electron diffraction (SAED) pattern indicating sharp rings, which reveals the polycrystalline nature of the nanoparticles.

*SEM analysis*

From the SEM pictures in Figure 5, randomly distributed nano-sized homogenous grains with some agglomerations are noticeable. The EDX spectrum of  $\text{Ni}_{0.25}\text{Co}_{0.75}\text{Fe}_2\text{O}_4$  nanoparticles is presented in Figure 6, which furnishes the chemical compositional analysis of the nanoscale  $\text{Ni}_{0.25}\text{Co}_{0.75}\text{Fe}_2\text{O}_4$ .

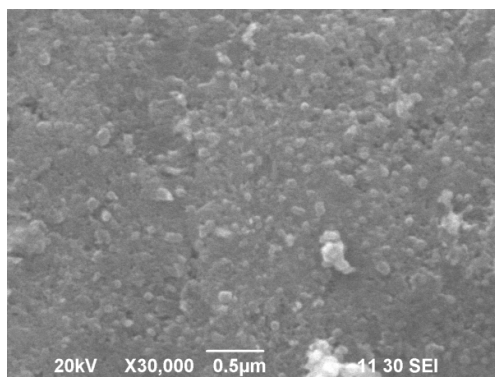


Figure 5. SEM image of  $\text{Ni}_{0.25}\text{Co}_{0.75}\text{Fe}_2\text{O}_4$  nanoparticles.

*EDX analysis*

The compositional data from the EDX analysis agree well with the theoretically calculated values, indicating a good compositional homogeneity across the nanoparticles.

Element	Percentage composition
Co	22.22
Ni	9.29
Fe	40.90
O	27.39

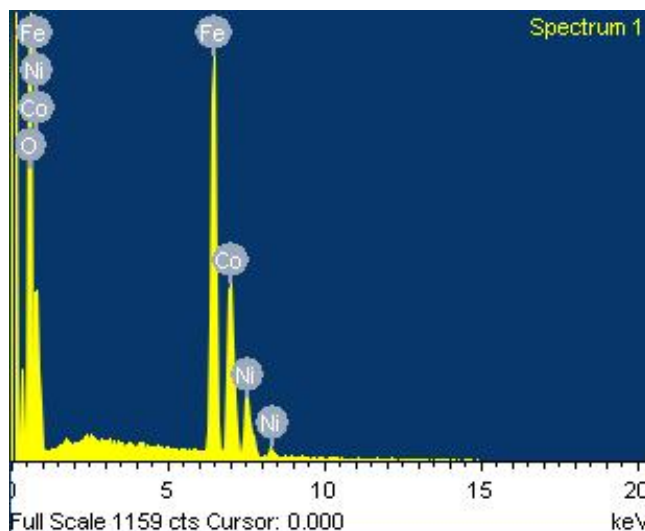


Figure 6. EDX spectrum of  $\text{Ni}_{0.25}\text{Co}_{0.75}\text{Fe}_2\text{O}_4$  nanoparticles.

### CONCLUSION

$\text{Ni}_{0.25}\text{Co}_{0.75}\text{Fe}_2\text{O}_4$  nanoparticles were successfully synthesised by a convenient thermal decomposition route and characterised by XRD, HRTEM, SAED and SEM techniques. The XRD pattern confirms the phase formation of  $\text{Ni}_{0.25}\text{Co}_{0.75}\text{Fe}_2\text{O}_4$ . The average size of 11 nm of  $\text{Ni}_{0.25}\text{Co}_{0.75}\text{Fe}_2\text{O}_4$  nanoparticles determined from HRTEM has no conflict with the XRD results. Overall, this method is found to be simplistic, commercially feasible and efficient in terms of time and equipment. Hence this forms an economical route for the mass production of ultrafine  $\text{Ni}_{0.25}\text{Co}_{0.75}\text{Fe}_2\text{O}_4$  powder.

### REFERENCES

1. Valenzuela, R. *Phys. Res. Int.* **2012**, DOI:10.1155/2012/591839.
2. Gedam, N.N.; Padole, P.R.; Rithe, S.K.; Chaudhari, G.N. *J. Sol-Gel Sci. Technol.* **2009**, *50*, 296.
3. Harris, V.G. *IEE Trans. Magn.* **2012**, *48*, 1075.
4. Gedam, N.N.; Padole, P.P.; Rithe, S.K.; Chaudari, G.N. *J. Sol-Gel Sci. Technol.* **2009**, *50*, 296.
5. Maaz, K.; Khalid, W.; Mumtaz, A.; Hasanain, S.K.; Liu, J.; Duan, J.L. *Phys. E.* **2009**, *41*, 593.
6. Qi, Y.L.; Yang, Y.S.; Zhao, X.F.; Liu, X.; Wu, P.; Zhang, F.; Xu, S. *Particuology* **2010**, *8*, 207.
7. Zhao, L.J.; Zhang, H.J.; Xing, Y.; Song, S.Y.; Yu, S.Y.; Shi, W.D.; Guo, X.M.; Yang, J.H.; Lei, Y.Q.; Cao, F. *J. Solid State Chem.* **2008**, *181*, 245.
8. Tanga, Y.; Wang, X.; Zhang, Q.; Li, Y.; Wang, H. *Prog. Nat. Sci.: Mater. Int.* **2012**, *22*, 53.
9. Randhawa, B.S.; Kaur, S.; Bassi, P.S. *J. Therm. Anal. Calorim.* **1999**, *55*, 789.
10. Gajapathy, D.; Patil, K.C.; Pai Vernekar, V.R. *Mater. Res. Bull.* **1982**, *17*, 29.
11. Randhawa, B.S.; Dosanjh, H.S.; Kumar, N. *J. Therm. Anal. Calorim.* **1999**, *95*, 75.
12. Khalil, I.; Petit-Ramel, M.M. *J. Inorg. Nucl. Chem.* **1979**, *41*, 711.

13. Sivasankar, B.N. *J. Therm. Anal. Calorim.* **2006**, 86, 385.
14. Sivasankar, B.N.; Govindrajan, S. *J. Therm. Anal.* **1997**, 48, 1401.
15. Rane, K.S.; Verenkar, V.M.S. *Bull. Mater. Sci.* **2001**, 24, 39.
16. Randhawa, B.S.; Kaur, M. *J. Therm. Anal. Calorim.* **2007**, 89, 251.
17. Gawas, U.B.; Mojumdar, S.C.; Verenkar, V.M.S. *J. Therm. Anal. Calorim.* **2009**, 96, 49.
18. Gonsalves, L.R.; Verenkar, V.M.S.; Mojumdar, S.C. *J. Therm. Anal. Calorim.* **2009**, 96, 53.
19. More, A.; Verenkar, V.M.S.; Mojumdar, S.C. *J. Therm. Anal. Calorim.* **2008**, 94, 63.
20. Sinduja, C.R.; Kalpanadevi, K.; Manimekalai, R. *Int. J. Sci. Res.* **2013**, 2, 64.
21. Jeffery G.H.; Bassett, J.; Mendham, J.; Denney, R.C. *Vogel's Textbook of Quantitative Chemical Analysis*, 5th Ed., Longman: UK; **1989**.
22. Braibanti, A.; Dallavalle, F.; Pellinghelli, M.A.; Leporati, E. *Inorg. Chem.* **1968**, 7, 1430.
23. Kambale, R.C.; Shaikh, P.A.; Kamble, S.S.; Kolekar, Y.D. *J. Alloys Compd.* **2009**, 478, 599.
24. *Natl. Bur. Stand. (U.S.) Monogr.* **1971**, 25/9, 22.
25. Subramanyam, K.N. *J. Phys. C: Solid State Phys.* **1971**, 4, 2266.